J. Phys. B: At. Mol. Opt. Phys. **24** (1991) 3685–3699. Printed in the UK

Bound states using the R-matrix method: Rydberg states of HeH

Baljit K Sarpal†, Susan E Branchett†, Jonathan Tennyson† and Lesley A Morgan‡

† Department of Physics and Astronomy, University College London, London WC1E 6BT, UK

‡ Computer Centre, Royal Holloway and Bedford New College, Egham, Surrey TW20 0EX, UK

Received 14 March 1991, in final form 29 May 1991

Abstract. A method is presented for adapting scattering calculations performed with the molecular R-matrix method to find bound states based on the atomic method of Seaton. Quantum defect theory is used to determine initial energy grids and to determine whether all the bound states have been located. This method is particularly suited to the Rydberg states of electron plus molecular ion systems. We calculate and assign the lowest 33 electronic states of the HeH molecule. Previously only 14 of the lowest ($n < 5$) bound states have been fully characterized, with several states omitted. We suggest that the omitted states give rise to some of the observed but previously unexplained weak transitions. Vibrational motion is included in our calculations within the adiabatic approximations. Effects arising from short-range correlations and nuclear motion are shown to be very significant for the lowest electronic states. Transition energies amongst the excited states agree with accurate spectroscopic determinations to better than 50 cm^{-1}.

1. Introduction

Over the last twenty years quantum chemists have developed powerful methods for treating the electronic states of small molecules. These methods are based on the use of a linear combination of atomic orbitals, Gaussian-type orbitals (GTO) and configuration interaction (CI) to represent electronic correlation effects. However, while such methods have proved very successful for compact, low-lying electronic states, they are less appropriate for the diffuse Rydberg states found below the ionization limit of all molecular species. Recently attempts have been made to adapt GTO expansions to Rydberg series (Kaufmann *et al* 1989). In this article we propose an alternative and, we would suggest, a more natural method of treating this problem.

The R-matrix method, although originally designed for scattering calculations, has been shown to yield a suitable framework (under appropriate boundary conditions) for determining atomic bound states (Seaton 1985). It has been successfully applied to atomic ions by Berrington and Seaton (1985) and Vo Ky Lan (1991). This procedure has recently been used as the basis for the Opacity Project (Seaton 1987, Berrington *et al* 1987) which involved the determination of very large numbers of atomic ion bound states. This method has an advantage over the quantum chemistry approach in that

0953-4075/91/173685+15$03.50

all the electronic states converging to a particular ionization threshold can in principle be determined once a suitable **R** matrix has been constructed. All that is needed is an algorithm for detecting these bound states.

Furthermore, within this formalism, the problem is transformed from trying simply to stabilize the high-lying states to one of trying to calculate increasingly small corrections due to electron–electron correlation effects and the long-range multipole potential in the outer region. To date molecular bound states have not been determined using the method used in this work. Indeed previous determinations of molecular bound states based on the method of Ojha and Burke (1983) were limited to bound states close to the R-matrix poles. This meant that it was only possible to detect a few low-lying states, for example see the work of Tennyson (1988) on the bound states of CH.

In molecules for a detailed comparison with experiment one needs to include the effects of nuclear motion. These can be included by using the electronic bound state energies determined for fixed geometries to act as a potential for the nuclear motion (*adiabatic nuclei* or Born–Oppenheimer approximation). This is most easily done either by direct solution of the 1D nuclear Schrödinger equation or by fitting to a Morse curve so that the solutions can be analytically determined. However for Rydberg series vibrational and electronic separations will rapidly become similar in magnitude. Under these circumstances the separation of electronic and nuclear motion through the Born–Oppenheimer approximation may lead to significant inaccuracies. These effects can be incorporated using the method introduced by Schneider *et al* (1979). Here we restrict our calculations to the adiabatic nuclei approximation.

The high-lying Rydberg levels ($n \geqslant 4$) of the neutral HeH are known to have considerable impact on both the vibrational excitation cross sections (Sarpal *et al* 1991a) and dissociative recombination of the HeH^+ ion (Yousif and Mitchell 1989, Sarpal *et al* 1991b). An accurate knowledge of the energy levels of both species is therefore essential in determining the spectroscopy of the molecule and scattering properties of the ion.

The HeH^+ ion has been extensively studied both experimentally (Schopman and Los 1970, Bernstein 1974, Carrington *et al* 1981) and theoretically (Annex 1963, Peyerimhoff 1965, Peek 1973, Green *et al* 1974, 1978, Michels 1989). The literature on the neutral HeH molecule is sparse by comparison. This is due mainly to the fact that the ground state of HeH is repulsive except for the small van der Waals minimum at large separation, and therefore is difficult to observe experimentally. However the excited states of the molecule are bound to varying degrees and these have been observed (van der Zande *et al* 1986, Brooks *et al* 1987, Ketterle *et al* 1988, 1989). This has led to recent theoretical interest in the bound states of HeH (Theodorakopoulos *et al* 1984, Petsalakis *et al* 1987, 1990). Several of these states show considerable predissociation via a non-adiabatic mechanism and radiative decay of some of the levels is also known to be appreciable (Theodorakopoulos *et al* 1987, Petsalakis *et al* 1990).

Recently Ketterle (1989, 1990a, b, c, d) has carried out an extensive experimental investigation of HeH together with its isotopic variants and has determined some highly excited states. Although the lower states have been calculated to reasonable accuracy, a theoretical treatment of the high Rydberg members for the neutral molecule is lacking. The most recent theoretical results of van Hemert and Peyerimhoff (1991) give good results in comparison with experiment, but are limited to the lowest 10 states. A considerable improvement of calculated vibrational and rotational energy levels is attained by a semi-empirical rescaling of potential energy curves and thresholds.

Although such a procedure is well justified for the case of HeH, it would be difficult to apply in a general case.

In section 2 we outline the theory on which the bound state detecting code (Branchett 1991) is based. This method is then applied to the specific case of HeH, the construction of the wavefunctions is described in section 3. The results and discussion are given in sections 4 and 5 respectively.

2. Theory

The R-matrix method considers a system of N tightly bound electrons which interact with an incident (continuum) electron. Asymptotically ($r_{N+1} \rightarrow \infty$, where $\boldsymbol{r}_{N+1}$ is the coordinate of the continuum electron relative to the target centre of mass) the incident electron experiences only a multipole-type potential. In this region the system can be treated analytically requiring the solution of a set of coupled second order differential equations. The interaction close to the target molecule must account for exchange within the $(N+1)$-electron system and electron–electron correlation. In the R-matrix method this region is defined as a sphere of radius a enclosing all target electrons. A detailed discussion of the R-matrix method is given by Gillan *et al* (1987) and we will restrict our discussion to points pertaining to finding bound states of the $(N+1)$-electron system.

The wavefunction of the $(N+1)$-electron system in the inner region is given as

$$\psi_k = \mathcal{A} \sum_{i,j} \phi_i(\boldsymbol{x}_1 \ldots \boldsymbol{x}_N) u_{ij}(\boldsymbol{x}_{N+1}) a_{ijk} + \sum_i \chi_i(\boldsymbol{x}_1 \ldots \boldsymbol{x}_{N+1}) b_{ik} \tag{1}$$

where $\boldsymbol{x}_n = (\boldsymbol{r}_n, \sigma_n)$ is the space–spin coordinate and for compactness $\boldsymbol{r}_{N+1}$ will be referred to as $\boldsymbol{r}$ from hereon. In (1) the sum over i allows for the inclusion of more than one target state, ϕ_i, and N is the number of target electrons. $\mathcal{A}$ is the anti-symmetrization operator; χ_i are configurations constructed from the target molecular orbitals which allow for short-range correlation and polarization effects, and u_{ij} are continuum orbitals. These u_{ij} are expanded as a partial wave expansion and the radial part is a solution of a 1D Schrödinger equation using a suitable potential. The continuum orbitals are generated subject to the boundary conditions

$$\left.\frac{\mathrm{d}u_{ij}}{\mathrm{d}r}\right|_{r=a} = \beta u_{ij} \tag{2}$$

$$u_{ij}(0) = 0 \tag{3}$$

where β is an arbitrary constant. The continuum orbitals are then Schmidt, and if necessary Lagrange (Tennyson *et al* 1987), orthogonalized to the occupied and virtual N-electron molecular orbitals retained in the calculation.

The variational coefficients a_{ijk} and b_{ik} in (1) are determined by diagonalizing $H_{N+1} + L_{N+1}$ in the internal region so that

$$\langle \psi_k | H_{N+1} + L_{N+1} | \psi_{k'} \rangle = e_k \delta_{kk'} \tag{4}$$

where H_{N+1} is the electronic part of the Hamiltonian and L_{N+1} is the Bloch operator used to ensure that the Hamiltonian is Hermitian in the inner region. The eigenenergies, e_k, are referred to as the R-matrix poles.

To obtain the surface amplitudes, $w_{ik}(a)$, of the inner region wavefunctions it is necessary to transform the boundary amplitudes of the continuum orbitals, $u_{ij}(a)$. Transformations arise from both the orthogonalization to the target orbitals and diagonalization of the inner region Hamiltonian. Full details of this procedure are given by Gillan *et al* (1987).

The wavefunction of the total system in the inner region, Ψ_E, of energy E, can be expanded as a sum of the wavefunctions ψ_k

$$\Psi_E = \sum_k \psi_k C_{kE} \tag{5}$$

where C_{kE} are the bound state coefficients. With suitable normalization of the ψ_k, it can be shown (Seaton 1985) that the reduced radial functions of the added electron F_i satisfy the equation:

$$F_i(r) = \sum_{j=1}^{I} R_{ij}(E)\left(\frac{\mathrm{d}F_j}{\mathrm{d}r} - \beta F_j\right) \tag{6}$$

where I is the total number of asymptotic channels. $R_{ij}(E)$ is known as the **R** matrix and is determined at the R-matrix boundary by

$$R_{ij}(E) = \frac{1}{2a}\sum_k w_{ik}(a)(e_k - E)^{-1} w_{jk}(a) + \delta_{ij}\mathcal{B}_i \tag{7}$$

where $\mathcal{B}_i$ is the Buttle (1967) correction necessitated by the arbitrary boundary condition (2).

In the outer region, functions are required that tend to zero as r tends to infinity and which can be matched to the inner region functions at the R-matrix boundary. These were obtained by first using the Gailitis expansion (Noble and Nesbet 1984) at an appropriate radius and then propagating inwards by solving the asymptotic equations numerically, using the Runge–Kutta–Nystrom method. The functions were stored in the matrix P_{ij}.

By imposing suitable boundary conditions Seaton (1985) showed that

$$\sum_j \left[P_{ij} - \left(\sum_k R_{ik}(E) Q_{kj}\right)\right] X_j = \sum_j B_{ij} X_j = 0 \tag{8}$$

where

$$Q_{kj} = \frac{\mathrm{d}P_{kj}}{\mathrm{d}r} - \beta P_{kj} \tag{9}$$

where all matrices are evaluated at the R-matrix boundary ($r = a$). **X** is a column vector needed to find the bound state coefficients C_{kE} given by

$$C_{kE} = \sum_i \frac{w_{ik}}{(e_k - E)} \sum_j \left(\frac{\mathrm{d}P_{ij}}{\mathrm{d}r} - \beta P_{ij}\right) X_j. \tag{10}$$

Equation (8) can only be solved for discrete values of energy, the bound state energies, which can be found by searching for zeros of the determinant of $\mathbf{B}(E)$.

It can be seen from (7) that the **R** matrix, and hence the matrix **B**(E) in (8), is not clearly defined at energies close to the R-matrix poles. It is therefore necessary to perform the matrix manipulations described by Burke and Seaton (1984) which enable the **B**(E) matrix to be expressed in a form where only the last row, i.e. $i = I$, has energy dependent terms. This last row can then be multiplied by $(e_K - E)$, where K is the index of the R-matrix pole closest in energy to the total energy of the system, to remove any computational errors caused by the nearness of an R-matrix pole. In practice the value of K was determined by searching through the values of the R-matrix poles to find the pole closest in magnitude to E. The equations corresponding to (8) then become:

$$\sum_{i'=1}^{I} L_{ii'} X_{i'} = 0 \qquad \text{for } i = 1 \text{ to } (I-1) \tag{11}$$

and

$$\sum_{i'=1}^{I} [L_{Ii'} - (e_K - E)^{-1} \Gamma^2 M_{Ii'}] X_{i'} = 0 \tag{12}$$

where L is given by

$$L_{ij} = \sum_k U^T_{ik} \left[P_{kj} - \left(\sum_l T_{k,l} Q_{lj} \right) \right] \tag{13}$$

T is given by

$$T_{ij}(E) = \frac{1}{2a} \sum_{k \neq K} w_{ik} (e_k - E)^{-1} w_{jk} \tag{14}$$

and M, U^T and Γ are defined in Burke and Seaton (1984).

In the atomic case there are only a small number of bound states associated with each value of principal quantum number n for a given total symmetry. However, for molecules this is not, in general, true. It was therefore necessary to introduce a method of searching for arbitrary numbers of bound state poles for a given value of the principal quantum number.

The search for zeros in the determinant of **B**(E) was carried out using a quantum defect grid. The effective quantum number n^* is given by (Seaton 1983)

$$n^* = n - \delta_n \tag{15}$$

where n is the principal quantum number and δ_n is the quantum defect. An equally spaced grid of effective quantum number was set up around the lowest value of the principal quantum number considered. The determinant of **B**(E) was then calculated at energies corresponding to the effective quantum number grid points. Zeros of the determinant were detected by a change in sign of the determinant from one grid point to the next. Where no change of sign was found a search for two poles between grid points was performed by fitting the determinant of **B**(E) to a quadratic function.

Setting up the **B** matrix at a particular energy and finding the determinant takes up a significant amount of computer time. An option was therefore implemented

to reduce the number of times that this was done: a fine grid of effective quantum numbers was set up in the regions where, assuming constant quantum defects for a Rydberg series, a state would be predicted by the calculations for lower n. A sparse grid was constructed in between these regions to determine new states, as at least one additional state (for each symmetry) appears for every increment of n.

Once the energy region of a bound state was found a Newton–Raphson search was performed to yield an approximate value for the bound state energy. The energy is assumed to be very close to the exact energy which is then calculated using the first two terms of a Taylor series expansion to obtain a standard eigenvalue problem:

$$\sum_j B_{ij}(E)X_j = \sum_j \left(B_{ij}(E_0) + (E - E_0)\frac{\mathrm{d}B_{ij}(E_0)}{\mathrm{d}r} \right) X_j = 0. \qquad (16)$$

This relation is used recursively until the required accuracy in E is achieved (see appendix 3 of Seaton 1985). This yields the bound state energy and eigenvector required to form the bound state wavefunction.

3. Details of the calculations

The target states, i.e. states of the HeH^+ ion, were constructed from the augmented $7 \times 5B$ basis of Peyerimhoff (1965) as defined by Sarpal *et al* (1991a). Only the lowest 6σ, 6π, 3δ and 1ϕ SCF orbitals, calculated using a modified version of the ALCHEMY package (McLean 1971, Noble 1982), were retained with the higher orbitals being discarded. The lowest three σ orbitals and the first π orbitals were used to construct CI wavefunctions of the three lowest states of the ion, $X\,^1\Sigma^+$, $a\,^3\Sigma^+$ and $A\,^1\Sigma^+$. Because the wavefunctions are a heavily truncated CI expansion, the absolute energies cannot be expected to be in agreement with more extensive expansion of the wavefunctions. However, as it is the relative energies which are amenable to experimental determinations, it is on these that we concentrate in this work. The relative energies of these target states were shown to be in good agreement with more extensive calculations (Green *et al* 1974, 1978, Sarpal *et al* 1991a).

As indicated earlier the continuum orbitals, u_{ij}, were expanded as a partial wave expansion. The radial functions were solutions of the 1D Schrödinger equations given by the isotropic part of the HeH^+ SCF potential and the boundary condition $\beta = 0$ with the R-matrix boundary set at $a = 10\ a_0$. We included all continuum orbitals having $l \leqslant 5$ and energies less than $5\ E_h$, which gave 57, 46, 36 and 26 numerical functions for the Σ, Π, Δ and Φ symmetries respectively. Such a high-energy cut-off is not necessary for the present work, but since we employ the same inner region wavefunction to carry out scattering calculations (Sarpal *et al* 1991a) we retained the same criteria.

The $(N+1)$-electron wavefunction is constructed, as defined by (1) (N is equal to 2 in our case), from the continuum and L^2 orbitals described above. As the target states are a reduced CI expansion it is important that correlation functions, χ, included in (1) to compensate for the relaxation of the orthogonalization constraint are consistent. A discussion of this is given by Sarpal *et al* (1991a). For the symmetries considered, Σ, Π, Δ and Φ, this resulted in an expansion of the $(N+1)$-electron wavefunction with 229, 240, 159 and 95 configurations respectively.

The asymptotic Gailitis expansion was applied at $r = 40\,a_0$ and then the functions propagated inwards to the R-matrix boundary at $10\,a_0$. The matrix manipulations and the bound state detecting algorithm, described in the last section, was then applied. For most cases it was sufficient to set up a grid of 20 points for the effective quantum numbers. For some of the higher angular momentum states it was necessary to increase this grid to 40 points.

4. Results

The bound states determined for the equilibrium separation of the HeH^+ ion are given in table 1. The quantum defects for the states are obtained from (15) where the effective quantum number is defined by

$$E_n(R) = E_\infty(R) - \frac{Z^2}{2(n^*(R))^2} \tag{17}$$

where E_n is the energy in Hartree, E_∞ is the energy of HeH^+ and $Z = 1$ for a HeH^+ target. The quantum defects for the bound states are in good agreement with the multichannel quantum defect (MCQD) parameters calculated just above the ionic threshold (Seaton 1983); these will be reported at a later date (Sarpal and Tennyson 1991). Also given in table 1 are the ionization potentials (IP), T_e, of the bound states. These have been calculated relative to the ground state energy of our HeH^+ at $-2.951\,208 E_h$. The calculated IP are compared with the experimental IP of Ketterle (1990d). The experimental energies are the differences between the minimum point energies of the different states which were deduced from spectroscopic data by Ketterle (1990d). Note that in table 1 we have labelled the electronic states using the *separated*-atom notation. Ketterle in his work uses the *united*-atom notation and therefore we have relabelled his C state from 3p Σ to 2p Σ. As our MCQD analysis discussed below demonstrates, the states in the HeH^+ equilibrium region are better described using the separated-atom limit.

The vertical transition energies derived from table 1 are in good agreement with experimental transition energies for higher members of the Rydberg series. For a more meaningful comparison with experiment than that provided in table 1, certainly for the lowest bound states, we must properly take into account that different potential energy curves will have different minimum points as well as different curvature. These effects arise from the complex interaction of the electron with the core electrons, which is represented by the correlation and polarization functions χ in (1).

The fixed nuclei calculations were carried out on a grid of 15 geometries ($R = 0.8$, 0.9, 1.0, 1.2, 1.3, 1.4, R_e=1.455, 1.5, 1.6, 1.8, 2.0, 2.4, 2.8, 3.0, 4.0 a_0). For the purposes of describing the potential energy curves most compactly we fitted our potential energy curves to a Morse function

$$V(R) = V_e + D\{1 - \exp[-\beta(R - R_e)]\}^2. \tag{18}$$

In the fitting procedure we found that the first two grid points have to be discarded in order to get the best fit near the minima for all potential energy curves. The accuracy of the Morse fit was $5 \times 10^{-4} E_h$. The parameters (in atomic units) for these fits are summarized in table 2 and the potential energy curves for the lowest 10 bound

Table 1. Bound states of neutral HeH with their quantum defects, δ, at equilibrium geometry of the ion, $R_e = 1.455\ a_0$. T_e is the energy in cm^{-1} relative to the ground state of the ion, $-2.951\ 208\ E_h$. The last column gives the ionization potentials deduced from experimental data by Ketterle (1990d).

Assignment†	Energy‡ (E_h)	δ	T_e (cm^{-1})	$T_e(expt)$ (cm^{-1})
1s $X\ ^2\Sigma$	−3.232 158	−0.334		
2s $A\ ^2\Sigma$	−3.094 013	0.129	31 339	31 695
2p $B\ ^2\Pi$	−3.080 895	0.036	28 460	28 888
2p $C\ ^2\Sigma$	−3.035 538	−0.435	18 506	18 837
3s $D\ ^2\Sigma$	−3.011 379	0.117	13 205	13 307
3p $E\ ^2\Pi$	−3.008 489	0.046	12 570	12 647
3d $F\ ^2\Sigma$	−3.007 627	0.023	12 381	12 430
3d $G\ ^2\Pi$	−3.007 228	0.012	12 294	12 355
3d $H\ ^2\Delta$	−3.006 284	−0.013	12 086	12 136
3p $^2\Sigma$	−2.993 210	−0.450	9 217	
4s $^2\Sigma$	−2.984 321	0.114	7 267	
4p $^2\Pi$	−2.983 156	0.044	7 011	7 058
4d $^2\Sigma$	−2.982 844	0.024	6 943	
4d $^2\Pi$	−2.982 665	0.013	6 903	6 931
4f $^2\Sigma$	−2.982 561	0.007	6 880	
4f $^2\Pi$	−2.982 537	0.005	6 875	
4f $^2\Delta$	−2.982 478	0.001	6 862	
4f $^2\Phi$	−2.982 351	−0.007	6 835	
4d $^2\Delta$	−2.982 263	−0.013	6 815	6 850
4p $^2\Sigma$	−2.976 391	−0.456	5 526	
5g? $^2\Delta$	−2.973 717	0.287	4 940	
5s $^2\Sigma$	−2.972 142	0.113	4 594	
5p $^2\Pi$	−2.971 571	0.045	4 469	
5d $^2\Sigma$	−2.971 411	0.025	4 434	
5d $^2\Pi$	−2.971 317	0.014	4 413	
5f $^2\Sigma$	−2.971 260	0.006	4 400	
5f $^2\Pi$	−2.971 248	0.005	4 398	
5g $^2\Pi$	−2.971 229	0.003	4 394	
5f $^2\Delta$	−2.971 211	0.000	4 390	
5g $^2\Sigma$	−2.971 208	0.000	4 389	
5g $^2\Phi$	−2.971 202	−0.001	4 388	
5d? $^2\Delta$	−2.971 200	−0.001	4 387	
5f $^2\Phi$	−2.971 155	−0.007	4 379	

† The $n = 5\ ^2\Delta$ states assignments are ambiguous, we have indicated this with a question mark on the relevant state.
‡ $1\ E_h = 2.194\ 746 \times 10^5 cm^{-1}$.

states, excluding the ground state, are given in figure 1. Also shown in figure 1 is the ionic threshold (dotted curve). These Morse curves were not used further in our work.

The vibrational energy levels listed in table 2 have been calculated by explicitly solving the 1D nuclear Schrödinger equation using the bound state energies, determined on the grid of 15 geometries, which were interpolated by fourth order polynomials (Le Roy 1971). The rotational constants, B_{rot}, were calculated from the expectation value $\langle R^{-2} \rangle$ of the lowest vibrational level for each electronic state.

Table 2. Parameters of a Morse fit to the potential energy curves ($1 \leqslant R \leqslant 4$). The energies of the vibrational levels has been obtained by numerical solution of the 1D Schrödinger equation. The energy of the lowest level is given in Hartrees, the higher levels are given relative to the lowest, in cm^{-1}. The rotational constant, B_{rot} (cm^{-1}) has been calculated from the expectation value (R^{-2}) for the lowest vibrational level for each electronic curve. B_{rot}^{exp}, Ketterle (1990d); B_{rot}^{vHP}, van Hemert and Peyerimhoff (1991).

	2s $A\,^2\Sigma$	2p $B\,^2\Pi$	2p $C\,^2\Sigma$	3s $D\,^2\Sigma$	3p $E\,^2\Pi$	3d $F\,^2\Sigma$	3d $G\,^2\Pi$	3d $H\,^2\Delta$	3p $^2\Sigma$	4s $^2\Sigma$
V_e	−3.09469	−3.08109	−3.03656	−3.01149	−3.00869	−3.00790	−3.00745	−3.00648	−2.99356	−2.98448
R_e	1.40396	1.45706	1.52548	1.45036	1.46553	1.46932	1.46883	1.46605	1.48566	1.46094
β	1.46405	1.41236	1.38624	1.44225	1.42265	1.40944	1.41496	1.42615	1.41193	1.42934
D	0.10557	0.09169	0.07724	0.08811	0.08676	0.08811	0.08706	0.08614	0.08330	0.08716
E_0	−3.08606	−3.07321	−3.02939	−3.00362	−3.00095	−3.00017	−2.99973	−2.99874	−2.98602	−2.97670
v_1	3512	3158	2788	3187	3083	3057	3070	3096	2981	3115
v_2	6726	6010	5288	6046	5854	5825	5834	5900	56	5910
v_3	9624	8548	7514	8552	8303	8307	8283	8392	8030	8371
B_{rot}	36.77	34.31	31.06	34.62	33.87	33.64	33.73	33.83	32.88	34.11
B_{rot}^{exp}	36.53	34.12	30.50	33.96	33.69	33.38	33.43	33.57		
B_{rot}^{vHP}	36.18	33.33	30.19	33.89	33.09	32.83	32.80	33.00	32.07	

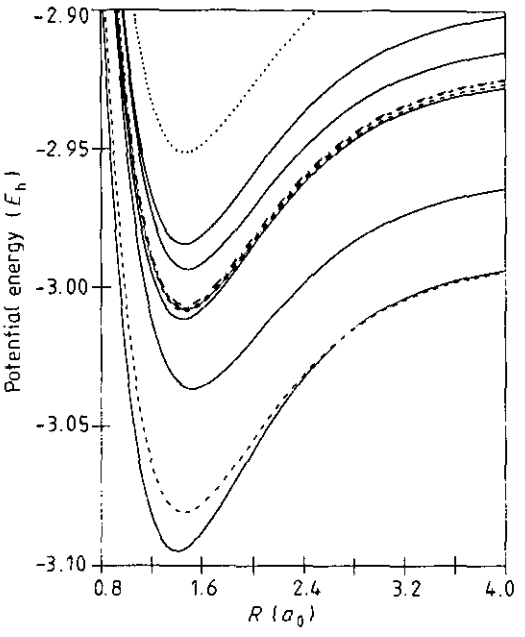

Figure 1. Potential energy curves for the lowest 10 bound states excluding the ground state; ——, Σ states; - - -, Π states; — · —, Δ state; · · · · · ·, ionic threshold ($X\ ^1\Sigma^+$).

5. Discussion

We find that, for the lowest few bound states, retaining only the *Coulomb term in* the outer region potential does not result in a significant error in the energy of these states. This is appreciated most easily by noting that for the lowest bound states the charge distribution is almost entirely enclosed within the R-matrix sphere, hence the potential in the outer region does not affect them significantly. The situation is not so for the higher levels which have appreciable amplitude outside the R-matrix sphere and are therefore responsive to the potential in the outer region. For these states it was necessary to retain *up to the quadrupole term in* the outer region potential in order to obtain converged results.

In table 1 we list several states which have not been determined previously. In fact some of these bound states would produce transitions which may have been observed already but could not be identified completely (Ketterle 1990d). Ketterle's analysis of his experimental data concentrated on the more intense transitions between lower states. The predictions for the higher lying states given here should help in the assignment of weaker unassigned transitions. It is notable that the difference between the states 2s $A\ ^2\Sigma$ and 2p $B\ ^2\Pi$ is approximately equal to that between the 3d $G\ ^2\Pi$ state and 3p $^2\Sigma$. This means that both 3d $G\ ^2\Pi$ — 2s $A\ ^2\Sigma$ and 3p $^2\Sigma$ — 2p $B\ ^2\Pi$ have approximately equal transition energies (~19 000 cm^{-1}) and one might expect further lines in this region. However, the new transitions are likely to be much weaker (Ketterle 1991).

We use the energies given in tables 1 and 2 to construct a table of transition energies, table 3. The relative separation amongst the E, F, G and H levels agrees with experimental determination of Ketterle (1990b) to within 20 cm^{-1}. Indeed energy

Table 3. Energy separations between some of the lowest bound states of HeH; a comparison with experiment (Ketterle 1990d) and theory (van Hemert and Peyerimhoff 1991). The theoretical separations are given relative to the experimental values of column 2. Energies in cm^{-1}.

		Theory (fixed R)†		Theory (adiabatic)	
Δ_{i-j}	Expt	vHP	This work	vHP	This work
A→B	2 563	−310	−316	−359	−257
A→C	12 427	33	−405	164	−11
A→D	18 215	149	81	130	122
A→H	19 249	−2	−3	1	85
B→C	9 864	343	−90	523	247
B→F	16 383	394	304	451	353
C→D	5 788	116	487	−34	132
C→H	6 822	−35	402	−163	95
D→E	547	−165	−87	−133	−39
D→F	731	−65	−92	−38	−26
D→G	808	−121	−103	−83	−46
D→H	1 034	−150	−84	−129	−37
E→F	184	100	−5	95	13
E→G	261	44	−16	50	−7
E→H	487	15	3	4	2
F→G	77	−56	−11	−45	−20
F→H	303	−85	8	−91	−11
G→H	226	−29	19	−46	9

† Our fixed R results are calculated for $R = 1.455\ a_0$ whereas van Hemert and Peyerimhoff's results are for $R = 1.5\ a_0$.

separations between any two levels, which do not include the A, B or C state (see below for these exceptions) agree to within 50 cm^{-1}, which is exceptional accuracy for *ab initio* calculations. Our higher energy levels are, without exception, in better agreement with experiment than previous theoretical calculations. Taking transition energies for all states between the A to II states we find that our results reproduce Ketterle's (1991d) experimental energies with a standard deviation of 174 cm^{-1} and a systematic mean error of 90 cm^{-1}. The corresponding numbers for the results of van Hemert and Peyerimhoff (1991) are 227 and 60 cm^{-1} respectively. We note that the major contribution to our errors arise from the uncertainty in the lower three state states (A, B and C). Excluding these states we find that our results are significantly better than other theoretical calculations. Also our rotational constants are in better agreement with experiment than the *ab initio* results of van Hemert and Peyerimhoff (1991).

Table 3 shows clearly that nuclear motion effects are very important, certainly for the lowest bound states, for a correct determination of transition energies. Also from table 3 one can deduce that the state $A\,^2\Sigma$ and $C\,^2\Sigma$ is too high in energy by $\sim 100\ cm^{-1}$ and $B\,^2\Pi$ is too high by $\sim 350\ cm^{-1}$. The probable reason for this differential in accuracy for these lower states is that as these states are the most compact, electron–electron correlation is very important, indicating perhaps that we have not treated these effects sufficiently accurately.

In figure 2 we plot the effective quantum numbers for the lowest 10 $^2\Sigma$ states as a function of internuclear separation. This type of plot has an advantage over the potential energy curves, figure 1, in that the energy scale is linearized so that

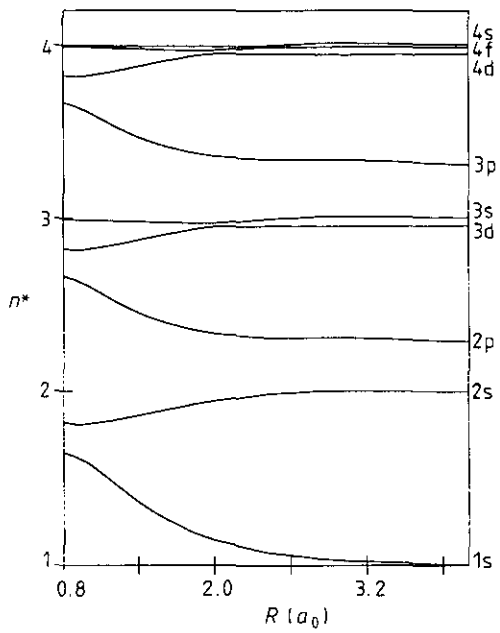

Figure 2. Effective quantum numbers, n^*, of the Σ symmetry bound states of HeH as a function of internuclear separation. The correlating state of hydrogen is indicated at large R.

interaction between states, which appear as avoided crossings, are most graphically displayed.

In figure 2 one observes a systematic repetition of the diagram, apart from the obvious appearance of an additional state as the principal quantum number increases by unity. This suggests that the electronic states are well behaved with a few avoided crossings at large internuclear separation. This also indicates that all the states are composed of a single core with a diffuse excited electron. The curve crossings, the first being between the $D\,^2\Sigma$ and $F\,^2\Sigma$ states at $R \sim 2.0\ a_0$, indicate mixing of states which may be very localized if the crossing is sharp or global if the avoided crossing is long range. The quantum defects for the higher symmetries are almost constant, apart from localized avoided crossings at $R \sim 2\ a_0$, and for this reason have not been plotted as a function of R. The values of the quantum defects for the higher symmetries are much smaller than those for the Σ symmetry.

An interesting feature of the plot in figure 2 is the particularly large quantum defect, ~ 0.5, for $np\ ^2\Sigma$ series. This arises from the fact that the principal quantum number of the lowest state differs by one depending on whether the two nuclei are separated (He + H) or united (Li). This results in the strong interaction of the $ns\ ^2\Sigma$ and $np\ ^2\Sigma$ at small internuclear separations. Indeed our MCQD calculations predict a swap over in l character near $R = 0.9\ a_0$. For values of R close to the equilibrium value for the ion ($1.455\ a_0$) the $ns\ ^2\Sigma$ and $np\ ^2\Sigma$ states are a 90% and 10% mixture, the lower of the two states corresponding to dominant s character. This is in agreement with Ketterle's (1990b) observation about the A state from intensity arguments and theoretical calculations of van Hemert and Peyerimhoff (1991). This will be considered in more detail in a later publication (Sarpal and Tennyson 1991).

An important implication of the R dependent character of an electronic state is that it may offer an insight into precisely where a radiative transition takes place. For example a $p\Pi \rightarrow p\Sigma$ transition is less favourable than $p\Pi \rightarrow s\Sigma$ (Petsalakis *et al* 1987), so that by changing R the transition can be turned on and off. This type of behaviour may become important for higher vibrational and rotational states whose mean internuclear separation is significantly different from the equilibrium value, resulting in intensity fluctuations in the vibrational and rotational bands.

For large internuclear separations, the low Rydberg states are probably not best described by functions centred on the centre-of-mass of the molecule and the quantum defects of these states for large internuclear separations should be considered in that light. For the higher Rydberg states the average size of the excited orbital is an order of magnitude larger than the internuclear separation, and the QDT analysis is applicable for these states. Of course if the basis set in which the wavefunction is expanded is sufficiently large, then it does not matter where the orbitals are centred.

The MCQD parameters, obtained by extrapolating through threshold in HeH^+ scattering calculations, were found to be in agreement with the $n = 5$ Rydberg states to within 0.002. The observation that the bound state quantum defects are so similar to the MCQD parameters, in magnitude as well as the variation with R, even for $n \geqslant 3$ is indeed a very powerful result. Specifically, it means that one has completely characterized all the bound states with $l \leqslant 5$ and up to Φ symmetry converging to the first ionic threshold. As the bound states associated with higher ionic thresholds all occur above the first threshold, avoided crossings with the Rydberg series do not occur. This results in nearly constant (but R dependent) quantum defects. The polarization effect of the Rydberg series converging to the next two thresholds is also included in our calculations as we retain the excited $a^3\Sigma$ and $A\,^1\Sigma$ target states of HeH^+ in our expansion of the inner region wavefunction, (1).

6. Conclusions

We have calculated the lowest 33 electronic bound states of HeH. Our results are both extensive and give better transition frequencies than previous *ab initio* determinations. We hope that this might lead to assignment of some of the weak transitions observed by Ketterle (1990d).

In our calculations the vertical (fixed equilibrium geometry) transition frequencies for the higher states are very similar to those where nuclear motion has been included. This is because the bound states are Rydberg in character and hence the potential energy curves are almost parallel to one another. The inclusion of zero point energy does not affect the relative energy levels significantly; the minimum for all states occurring for the same value of R. It is for similar reasons that the excitation energies are isotope independent, as the differences in zero point energy, which are due to the different reduced mass, shift uniformly.

Although the accuracy of our calculations are below the final results of van Hemert and Peyerimhoff (1991), it should be noted that we do not apply any rescaling of potential energy curves and thresholds. Indeed if *ab initio* results are compared then our results are significantly better than any previous work. It should be possible to get increased accuracy by improving our target wavefunctions, this procedure would still involve far fewer configurations than the standard quantum chemistry approach.

The level of agreement between our electronic transition energies and the experimental measurements demonstrates the advantage of the *R*-matrix method in determining diffuse bound states. We believe that this method will prove to be of significant value for the understanding of molecular Rydberg states. The main advantage stems from the method being able to treat both the scattering and bound state phenomenon in a unified manner and more importantly to the same accuracy. These points are also important for the interpretation of resonances at low scattering energies (Sarpal *et al* 1991a). Furthermore the number of configurations employed in the *R*-matrix method is significantly smaller than those required for a quantum chemistry calculation of similar accuracy. Work is currently in progress on developing a code to calculate transition moments between diffuse states of the type considered here (Branchett 1991). Calculations are also in progress on dissociative states of HeH in order to study dissociative recombination of HeH^+ plus an electron (Sarpal *et al* 1991b) where the bound states of the neutral play an important role.

Acknowledgments

We thank Dr Peter Storey for helpful discussions during the course of this work and Dr Ketterle for his comments on our manuscript. We thank Dr Ketterle and Professor Peyerimhoff for supplying copies of their work prior to publication. This work was supported by SERC grant GR/F/14550.

References

Annex B G 1963 *J. Chem. Phys.* **38** 1651–62
Bernstein R B 1974 *Chem. Phys. Lett.* **25** 1–8
Berrington K A, Burke P G, Butler K, Seaton M J, Storey P J, Taylor K T and Yu Yan 1987 *J. Phys. B: At. Mol. Phys.* **20** 6379–97
Berrington K A and Seaton M J 1985 *J. Phys. B: At. Mol. Phys.* **18** 2587–99
Branchett S E 1991 *PhD Thesis*, London University to be submitted
Brooks R L, Hunt J L and Miller J J 1987 *Phys. Rev. Lett.* **58** 199–202
Burke P G and Seaton M J 1984 *J. Phys. B: At. Mol. Phys.* **17** L683–7
Buttle P J A 1967 *Phys. Rev.* **160** 719–29
Carrington A, Buttenshaw J, Kennedy R A and Softley T P 1981 *Mol. Phys.* **44** 1233–7
Gillan C J, Nagy O, Burke P G, Morgan L A and Noble C J 1987 *J. Phys. B: At. Mol. Phys.* **20** 4585-603
Green T A, Michels H H, Browne J C and Madsen M M 1974 *J. Chem. Phys.* **61** 5186–97
Green T A, Michels H H, and Browne J C 1978 *J. Chem. Phys.* **69** 101–5
Kaufmann K, Baumeister W and Jungen M 1989 *J. Phys. B: At. Mol. Opt. Phys.* **22** 2225–40
Ketterle W 1989 *Phys. Rev. Lett.* **62** 1480–3
—— 1990a *J. Chem. Phys.* **93** 3752–9
—— 1990b *J. Chem. Phys.* **93** 3760–72
—— 1990c *J. Chem. Phys.* **93** 6929–34
—— 1990d *J. Chem. Phys.* **93** 6935–41
—— 1991 Private communication
Ketterle W, Dodhy A and Walther H 1988 *J. Chem. Phys.* **89** 3442–53
Ketterle W, Messmer H P and Walther H 1989 *Phys. Rev.* A **40** 7434–7
Le Roy R J 1971 *J. Chem. Phys.* **54** 5433–4
McLean A D 1971 *Conf. Potential Energy Surfaces in Chemistry* ed W A Lester Jr (San Jose: IBM Research Laboratory) p 87
Michels H H 1989 *Dissociative Recombination: Theory, Experiment and Applications* ed J B A Mitchell and S L Guberman (Singapore: World Scientific) pp 97–108

Noble C J 1982 *Daresbury Laboratory Technical Memorandum* DL/SCI/TMT33T
Noble C J and Nesbet R K 1984 *Comput. Phys. Commun.* **33** 399–411
Ojha P C and Burke P G 1983 *J. Phys. B: At. Mol. Phys.* **16** 3513–29
Peek J M 1973 *Physica* **64** 93–113
Petsalakis I D, Theodorakopoulos G, Nicolaides C A and Buenker R J 1987 *J. Phys. B: At. Mol. Phys.* **20** 5959–65
Petsalakis I D, Theodorakopoulos G and Buenker R J 1990 *J. Chem. Phys.* **92** 4920–3
Peyerimhoff S D 1965 *J. Chem. Phys.* **43** 998–1010
Sarpal B K and Tennyson J 1991 to be published
Sarpal B K, Tennyson J and Morgan L A 1991a *J. Phys. B: At. Mol. Opt. Phys.* **24** 1851–66
—— 1991b to be published
Schneider B I, Le Dourneuf M and Burke P G 1979 *J. Phys. B: At. Mol. Phys.* **40** L365–9
Schopman J and Los J 1970 *Physica* **48** 190–216
Seaton M J 1983 *Rep. Prog. Phys.* **46** 167–257
—— 1985 *J. Phys. B: At. Mol. Phys.* **18** 2111–31
—— 1987 *J. Phys. B: At. Mol. Phys.* **20** 6363–78
Tennyson J 1988 *J. Phys. B: At. Mol. Opt. Phys.* **21** 805–16
Tennyson J, Burke P G and Berrington K A 1987 *Comput. Phys. Commun.* **47** 207–12
Theodorakopoulos G, Farantos S C, Buenker R J and Peyerimhoff S D 1984 *J. Phys. B: At. Mol. Phys.* **17** 1453–62
Theodorakopoulos G, Petsalakis I D, Nicolaides C A and Buenker R J 1987 *J. Phys. B: At. Mol. Phys.* **20** 2339–45
van der Zande W J, Koot W, de Bruijn D P and Kubach C 1986 *Phys. Rev. Lett.* **57** 1219–22
van Hemert M C and Peyerimhoff S D 1991 *J. Chem. Phys.* **94** 4369–83
Vo Ky Lan 1991 *J. Phys. B: At. Mol. Opt. Phys.* **24** 833–48
Yousif F B and Mitchell J B A 1989 *Phys. Rev.* A **40** 4318–21